

Characterization of NU-LHT-4M Lunar Regolith Simulant Using Different Raman Configurations.

Eric Z. Tucker¹, M. Nurul Abedin¹, Russell A. Wincheski¹, and Douglas Rickman², ¹NASA Langley Research Center, Hampton, Virginia 23681, USA, E-mail: [E-mail: Eric.Z.Tucker@nasa.gov](mailto:Eric.Z.Tucker@nasa.gov), ²Jacobs, Jacobs Space Exploration Group/NASA Marshall Space Flight Center, Huntsville, AL, 35812, USA.

Introduction: As much as possible, structures to help sustain a long-term human presence on the moon will be constructed via in-situ resource utilization (ISRU) from lunar regolith [1]. Various processes have been proposed to produce lunar regolith-based construction materials, but one complication is that the lunar regolith is relatively complex in terms of composition and can vary quite significantly from one site to another [2]. Some of these construction material processes are quite sensitive to the composition; therefore, in-situ methods for evaluating the composition of the lunar regolith could be critical [1,3]. Various analytical instrumentation has been proposed for in-situ characterization of the composition of regolith on planetary bodies [4,5]. Raman spectroscopy has been suggested and has some advantages over other in-situ techniques, such as potential for relatively high spatial resolution, direct determination of the mineralogy (while other methods may only infer the mineralogy), nondestructive analysis, relatively simple instrument configurations, and minimal sample preparation/handling [6]. Raman instrumentation has already been deployed in rover-based missions to Mars [7-9]. Previously, we developed the Standoff Ultracompact Micro-Raman Sensor (SUCR), which is a portable Raman spectroscopy instrument capable of integration onto a rover or lander [10,11]. Here, we present work on Raman spectroscopy measurements of NU-LHT-4M lunar simulant using three different Raman instruments with different configurations for collecting Raman data with the goal to explore the effect of these different configurations on the results, especially for use in a lunar environment.

Experimental Methodology: A lunar regolith simulant, NU-LHT-4M, was characterized using three different Raman instrument configurations: a confocal microscope-based commercial tabletop system, a similar commercial system that utilizes a fiber optic probe instead of a confocal microscope, and the Standoff Ultracompact Micro-Raman Sensor

(SUCR). In addition, the confocal microscope-based system was measured with both a 532 nm and 785 nm laser while the fiber optic probe-based system utilized a 785 nm laser for excitation. A description of the SUCR instrument is provided in previous work where a 532 nm laser is used for excitation. However, in this work the SUCR instrument configuration was modified to include a 10x objective lens in place of the previously used cylindrical lens [11]. In all cases the simulant was dispersed onto glass and different positions on the sample were measured to obtain multiple spectra.

Results: Plotted in Figures 1a and 1b are Raman spectra collected from different positions on the NU-LHT-4M simulant using the confocal microscope-based and fiber optic probe-based instruments, which both utilized a 785 nm laser. Here, peaks attributed to the plagioclase, pyroxene, and olivine groups of minerals, which are the main mineral constituents of the NU-LHT-4M simulant, were found and are labeled accordingly. Similar peaks were observed with the other configurations (not shown). Generally, as expected, data from the confocal microscope-based (Fig. 1a) and the SUCR (not shown) instruments, which both utilized a microscope objective to probe much smaller relative areas compared to the fiber optic probe system, showed significant variation in the Raman spectra point-by-point across different positions on the simulant sample. In contrast, the fiber optic probe-based system (Fig. 1b), which interrogates a larger area, showed consistent measured spectra across different positions on the sample and showed peaks from all the main mineral constituents in each spectrum while also enabling for measurement at greater standoff distances. Interestingly, peaks that are much broader and stronger than peaks attributed to Raman signals were observed at roughly 1200-1500 cm^{-1} , corresponding to the roughly 870-890 nm wavelength range, from many points using the confocal microscope-based and fiber optic probe-based instruments utilizing a 785 nm wavelength

laser for excitation (Figs. 1a and 1b). These pronounced peaks are not as clearly visible in the data from the SUCR instrument (not shown).

Conclusion: The configurations that enable smaller area measurements have the benefit of potentially being able to provide more quantitative information in terms of mineral composition through performing an analysis similar to other point-counting methods for determining mineral composition while the larger area method enabled by the fiber optic probe-based instrument provides higher throughput, but more of a qualitative indication of the mineralogy [12]. The exact origin of the strong peaks in the data from the confocal microscope-based and fiber optic probe-based instruments is currently being investigated.

Acknowledgements: The work here has been supported by the National Aeronautics and Space Administration (NASA).

References:

[1] Clinton R. G. et al. (2021) "Overview of NASA's Moon-to-Mars Planetary Autonomous Construction Technology (MMPACT)," in *ASCEND 2021*, Los Vegas. [2] Gustafson R. et al. (2007) "Development of high-fidelity lunar regolith simulants with agglutinates," in *Lunar and Dust Regolith Simulant Workshop*, Huntsville. [3] Hintze P. E. and Quintana S. (2013) "Building a Lunar or Martian Launch Pad with In Situ Materials," *J. Aerosp. Eng.*, *26*, 134-142. [4] Blake D. et al. (2012) "Characterization and calibration of the CheMin mineralogical instrument on Mars Science Laboratory," *Space Sci. Rev.*, *170*, 341-399. [5] Cloutis E. A. et al. (2015) "The Canadian space agency planetary analogue materials suite," *Planetary and Space Science*, *119*, 155-172. [6] Wang A. et al. (1998) "Prototype Raman Spectroscopic Sensor for in Situ Mineral Characterization on Planetary Surfaces," *Appl. Spectrosc.* *52*, 4, 477-487. [7] Bhartia R. et al. (2021) "Perseverance's scanning habitable environments with Raman and luminescence for organics and chemicals (SHERLOC) investigation," *Space Sci. Rev.*, *217*, 1-115. [8] Rull F. et al. (2017) "The Raman Laser Spectrometer for the ExoMars Rover Mission to Mars," *ASTROBIOLOGY*, *17*, 627-654. [9] Kloosterman J. et al. (2012) "First observations

with SuperCam and future plans," in *Millimeter, Submillimeter, and Far-Infrared Detectors and Instrumentation for Astronomy VI*, Amsterdam. [10] Abedin M. N. et al. (2016) "Ultra-Compact Raman spectrograph for planetary surface inspection," in *47th Annual Lunar and Planetary Science Conferenc.* [11] Abedin M. N. et al. (2018) "Standoff ultracompact micro-Raman sensor for planetary surface explorations," *Appl. Opt.*, *57*, 62-68. [12] Haskin L. A. et al. (1997) "Raman spectroscopy for mineral identification and quantification for in situ planetary surface analysis: A point count method," *J. Geophys. Res.*, *102*, 19293-19306.

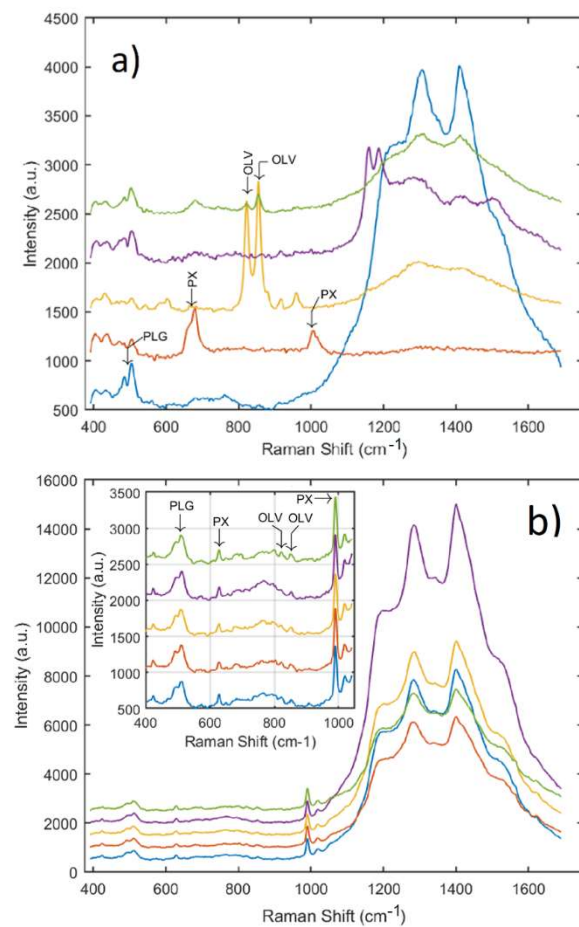


Fig. 1. Raman spectra showing measurements from different points on the NU-LHT-4M simulant sample using the (a) confocal microscope-based benchtop and (b) fiber optic probe-based instruments. Both instruments utilized a 785 nm excitation source. Individual spectra have been offset along the y-axis and background subtracted using a b-spline fit. Peaks labeled with PLG, PX, and OLV have been attributed to plagioclase, pyroxene, and olivine mineral groups, respectively.